Catena 223 (2023) 106964

Contents lists available at ScienceDirect

Catena

journal homepage: www.elsevier.com/locate/catena

What drives wind erosion in cropped areas? A case study in southern Tunisia

Christel Bouet [a,b,*], Mohamed Taieb Labiadh [c], Caroline Pierre [a], Saâd Sekrafi [c], Thierry Henry des Tureaux [a], Mohsen Ltifi [c], Gilles Bergametti [b], Béatrice Marticorena [d], Amadou Abdourhamane Touré [e], Jean Louis Rajot [a,b]

[a] iEES Paris (Institut d'Ecologie et des Sciences de l'Environnement de Paris), UMR IRD 242, Univ Paris Est Creteil - Sorbonne Université - CNRS - INRAE - Université Paris Cité, F-93143 Bondy, France
[b] Université Paris Cité and Univ Paris Est Creteil, CNRS, LISA, F-75013 Paris, France
[c] IRA (Institut des Régions Arides) de Médenine, El Fjé 4119, Tunisia
[d] Univ Paris Est Creteil and Université Paris Cité, CNRS, LISA, F-94010 Créteil, France
[e] Université Abdou Moumouni, Faculté des Sciences et Techniques, Département de Géologie, BP 10662 Niamey, Niger

ARTICLE INFO

Keywords:
Wind erosion
Hordeum vulgare L.
Growing season
Saltation flux
Aerodynamic roughness length
Tunisia

ABSTRACT

Dust emission by wind erosion is a worldwide phenomenon that threatens sustainable development and population wellness in areas where anthropogenic activities develop. However, uncertainties on the current estimates of dust originating from agricultural activities remain high. This study aims at disentangling the respective roles of meteorology, surface properties, and human practices in the dynamics of wind erosion over croplands. Therefore, an experimental field campaign was conducted in a traditionally cultivated barley field in southern Tunisia during the agricultural year 2015–2016. Meteorological parameters (wind speed and direction, rainfall), surface characteristics (barley surface cover and height), and the horizontal flux of aeolian sediments were measured. Land management was also documented. 97% of the wind erosion fluxes occurred between mid-May and November 2016. This was explained by the seasonal cycle of barley crop, land management, and meteorological conditions: (i) in autumn, the soil surface sufficiently wet to allow barley growth is tilled, which creates clods that increase the soil surface roughness and inhibits wind erosion, (ii) late winter coincides with the period of the highest wind speed but the height of the barley, maximal in this period, prevents wind erosion, and (iii) the field surface left bare and trampled at the end of harvest in spring is totally prone to wind erosion. This study highlights the importance of accounting for the joint seasonality of the meteorological parameters, vegetation cover, and human practices when studying wind erosion. Neglecting one of these parameters can induce a net overestimation/underestimation of wind erosion by the models.

1. Introduction

Wind erosion is the result of the entrainment of surface soil particles and of their deposit by wind. This natural phenomenon occurring mainly in the arid and semi-arid areas of the planet (Prospero et al., 2002) is modulated by both the climate (wind, precipitation) and soil surface properties (texture, soil size distribution, roughness, vegetation cover, etc) (Bagnold, 1941). In recent years, dust storms consecutive to wind erosion have become more frequent as a result of the climate change (Parolari et al., 2016; Zhang et al., 2018) and of the land surface modifications due to anthropogenic (e.g., political and socioeconomic) factors (Chi et al., 2019). They were identified as one of the emerging and hot topic consequences of climate change (Mirzabaev et al., 2019) that impact people and economic activities, particularly in the agricultural sector for which the interactions with the environment are numerous (Gholizadeh et al., 2021). Indeed, development of agricultural activities may increase wind erosion meanwhile suffering from it. As an example, Houyou et al. (2016) showed that, in the Algerian steppe, the conversion of native vegetation into cropland led to very large soil loss rates due to wind. Also, wind erosion can have large impacts on crop productivity, and consequently on farmers' income (Gholizadeh et al., 2021; Santra et al., 2017): it affects the crop yield directly by damaging

* Corresponding author at: LISA, 61, avenue du Général de Gaulle, 94010 Créteil Cedex, France.
E-mail address: christel.bouet@ird.fr (C. Bouet).

https://doi.org/10.1016/j.catena.2023.106964
Received 18 May 2022; Received in revised form 13 January 2023; Accepted 18 January 2023
Available online 23 January 2023

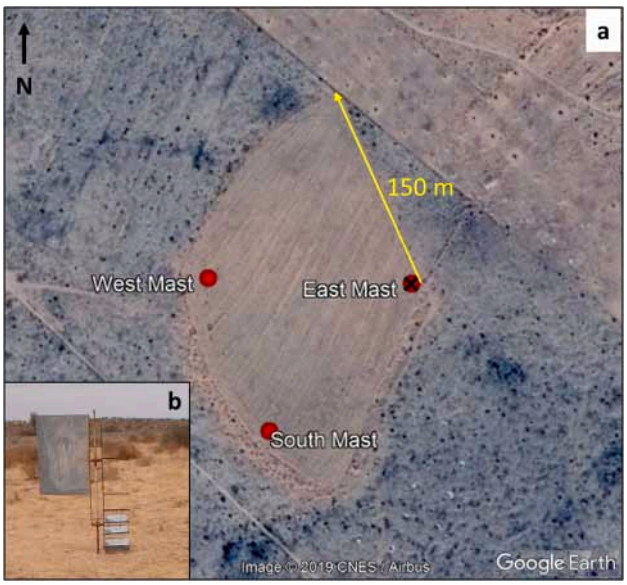

Fig. 1. (a) Google Earth Image (on 27/02/2016) of the experimental plot. Red dots locate the three masts equipped with BSNEs (b). The black cross locates the meteorological masts. (For interpretation of the references to colour in this figure legend, the reader is referred to the web version of this article.)

the plants through abrasion, burial, and deposition of dust on the leaves (Michels et al., 1995) that limits the incoming solar radiation available for photosynthesis (Squires, 2016), and indirectly by reducing soil fertility through loss of nutrients and thinning of the top soil (Larney et al., 1998). Thus, evaluating accurately the dynamics of wind erosion is important for controlling the risk of impoverishment of soils and dust emission. Several studies have demonstrated that agricultural practices also play an important role by controlling the temporal variability and magnitude of wind erosion (Lee et al., 1993; Pierre et al., 2018). For instance, Pierre et al. (2018) used a modelling approach to show that the variability of annual wind erosion fluxes induced by agricultural practices in the Central Sahel could be of the same order as the variability due to meteorological factors. As a consequence, an accurately evaluation of wind erosion dynamics in agricultural areas requires to document jointly the capacity of wind to erode the soil surface, the rain occurrence, surface properties, and the agricultural practices. Beyond the definition of land management practices that would limit wind erosion and its consequences on land resources, the interest of such studies is that they would help reduce the current uncertainties of the dust models as to the contribution of agricultural activities to the total atmospheric dust load. Indeed, the literature review conducted by Stanelle et al. (2014) concluded that the change of the today's total dust emissions attributable to human activities was comprised between −20 % and 60 %. As an example, using the same observational dataset (dust storm frequency data to constrain global dust model outputs), Tegen et al. (2004) concluded that the contribution of dust from agricultural areas to the global dust load was less than 10 %, whereas Mahowald et al. (2004) found that this contribution ranged between 0 and 50 %. More recently, using the dust optical depth Deep Blue product derived from the measurements of Moderate Resolution Imaging Spectroradiometer (MODIS) in conjunction with other data sets including land use, Ginoux et al. (2012) estimated that anthropogenic (primarily agricultural) sources accounted for 25 % of the global dust emissions. Furthermore, they estimated that 20 % of dust emissions originated from vegetated surfaces, primarily desert shrublands and agricultural lands. Finally, these authors concluded on the necessity of a better mapping of threshold wind velocities, vegetation dynamics, and surface conditions (soil moisture and land use) in order to improve dust emission estimates. Unfortunately, to date very few studies exist that document jointly all the parameters listed above for the regions where wind erosion threatens croplands (Nordstrom and Hotta, 2004).

Barley is a cereal widely cultivated worldwide (see for instance Marp 3 in Gholizadeh et al. (2021)), and included in most of the countries of the "dust belt" (an area that extends from the west coast of North Africa, through the Middle East, South and Central Asia, to eastern China). For instance, in Morocco, barley occupies, on average, 2.3 million hectares out of 5.2 million hectares annually planted with cereal crops (Ceccarelli et al., 2001). Similarly, in Tunisia, barley occupies about 0.5 million out of 1.5 million hectares planted annually with cereal crops. It is also the most favored cereal in the south of the country because of its adaptability to dryland (Slama et al., 2005).

In southern Tunisia, soils are sandy, precipitations scarce, and vegetation sparse. So, wind erosion is naturally very active (Khatelli and Gabriels, 2000), but the mechanization of agriculture has increased its impact (Akrimi et al., 1993). Consequently, southern Tunisia is an ad-hoc environment to assess the respective roles of meteorology and agricultural practices on wind erosion.

This study aims at documenting the impact of a crop cycle on wind erosion and at disentangling the respective roles played by meteorology, surface properties, and human practices. To do so, an experimental field campaign was conducted in southern Tunisia during agricultural year 2015–2016 on a barley field with a traditional land management. Meteorological parameters, in particular wind speed and direction and precipitation, as well as surface characteristics (including barley growth), and horizontal fluxes of aeolian sediments were measured. This data set is used to understand what controls wind erosion in the region and to propose possible improvements in the land management. In the future, this data set could also be used to improve wind erosion modeling in traditional cultivated areas of southern Tunisia so that the contribution of these areas to total dust emission could be estimated in this region.

2. Material and methods

2.1. Description of the field experiment

The experiment was carried out from 5 October 2015 to 11 November 2016 in the Dar Dhaoui experimental range (latitude 33°17′45″N, longitude 10°46′57″E) of the Institut des Régions Arides (IRA) of Médenine (Tunisia). The Dar Dhaoui experimental range has been used to study wind erosion processes for several decades (Dupont et al., 2019; Kardous, 2005; Khatelli, 1996, 1981; Labiadh et al., 2013). It is located in the arid region of the Jeffara Plain in south-east Tunisia. In this region, annual rainfall varies from 60 mm to the south to 220 mm near the coast and in the mountains (Ouessar et al., 2006). Rain is the most frequent from October to January, but quasi absent from May to August (Kallel, 2001). Active winds (wind speed larger than 3 m s^{-1} at 1.5 m height) occur mostly during winter and spring, from December to May (Khatelli and Gabriels, 2000). Soil size distribution can influence the wind erosion fluxes (Shahabinejad et al., 2019a, 2019b). In southern Tunisia, this soil size distribution was found to be remarkably homogeneous (Labiadh et al., 2011) with the ubiquitous and dominant presence of a very fine sand and well-sorted population (~100 μm in diameter). A secondary but minor population of coarse grains (1 500 μm) can be found, but only in the vicinity of mountains, thus at a distance of the study plot. On the selected site, the parent soil is aeolian fine sand deposit generally lying on calcrete (Labiadh et al., 2013), and the median diameter of the grain-size distribution of the soil surface is 90 μm (Khalfallah et al., 2020). This diameter corresponds to the soil grains for which the wind erosion threshold is minimum (Greeley and Iversen, 1985), which makes the soils of this region very prone to wind erosion.

During the experiment, a large third of a ~ 150 m radius circle plot (Fig. 1a) was traditionally cultivated (i.e., without irrigation nor fertilization) with barley (*Hordeum vulgare L.*, cultivar Ardhaoui – unique cultivar in southern Tunisia (Thameur et al., 2012)). After a rainfall of

Fig. 2. Photographs of (a) the barley sowing, (b) mechanical tillage of the field on 21/10/2015, and (c) the manual harvesting of barley on 20/04/2016.

30.8 mm on 16 October 2015, barley was sown on the fly (Fig. 2a) before the plot was tilled with a disc plough (Fig. 2b) on 21 October 2015. Harvest was done manually from 18 to 22 April 2016 (Fig. 2c): barley tufts were removed by hand to collect at the same time seeds, roots and straws, the latest being used as fodder for sheep. The plot was surrounded by small bushes to the East, West, and North-West and young olive trees arranged in a square pattern to the North-East (Fig. 1a).

2.2. Measurements of the micrometeorological parameters

2.2.1. Meteorological parameters

A mast equipped with 7 cup anemometers (A100R Vector Instrument®; resolution = ± 0.1 m s^{-1}) was set up at the eastern edge of the plot (Fig. 1a) to measure at 0.1 Hz the wind speed vertical profile. Data were acquired using a CR1000 data logger (Campbell® Scientific company), with a nominal data acquisition time of 1-min. The 7 anemometers were respectively set at 0.285 m, 0.825 m, 1.395 m, 1.920 m, 2.965 m, 4.060 m, and 5.005 m above ground level (AGL). These measurements allowed estimating the aerodynamic roughness length, z_0 (see §2.2.2.).

Additional wind speed and direction as well as rainfall measurements were continuously performed using a meteorological station located 10 m north of the meteorological mast. Wind speed and direction were measured there at 2 m AGL using a 2 dimensional (2D) sonic anemometer (WindSonic^{TM} Gill Instruments ltd), and rainfall using an ARG100 Tipping Bucket rain gauge (Campbell® Scientific company). Data were acquired using a CR200X data logger (Campbell® Scientific company), with a nominal data acquisition time of 5-min for all parameters measured with a frequency of 0.1 Hz. Given the high variability of both wind speed and direction on a 5-min time step, the maximum and mean values of wind speed, and the mean and standard deviation of wind direction measured over this interval were recorded. 5-min rainfall measurement corresponds to the accumulated bucket tippings over this interval with one tipping corresponding to 0.2 mm of rainfall.

2.2.2. Aerodynamic roughness length

The same methodology as that described in Pierre et al. (2015) was used to assess the aerodynamic roughness length. In near neutral atmospheric conditions, z_0 can be estimated by fitting a logarithmic law to the wind profile measured by the cup anemometers (Priestley, 1959):

$$u(z) = \frac{u_*}{k} ln \frac{z}{z_0} \quad (1)$$

with k the von Kármán constant ($k = 0.4$), z the height (in m) of measurement of wind speed $u(z)$ (in m s^{-1}) and u_* the friction velocity (in m s^{-1}). In this study, we used 15-min averages for wind speed following the results obtained by Dupont et al. (2018) on the same field who showed that this averaging time ensures that all significant turbulent structures carrying momentum flux are included. The aerodynamic roughness length was computed from linear regression of the wind profile described by Equation (1). To select near neutral conditions, only wind speeds recorded between 06:00 am and 08:30 am and between 04:30 pm and 07:00 pm in local time, i.e. during the sunrise and the sunset respectively, were retained. Moreover, the following criteria, adapted from Marticorena et al. (2006), were applied:

(i) computation of the aerodynamic roughness length was only done for wind directions with maximum fetch, that is between [210°, 330°] (Fig. 1a);
(ii) in order to avoid free convection, regression was only computed if wind speed at all heights was greater than 1 m s^{-1}, and the result of the regression was retained only if u_* from the regression was greater than 0.1 m s^{-1};
(iii) the result of the regression was retained if the difference between measured and fitted wind speeds was lower than 5 % at all heights. Since the agreement between measured and fitted wind

Table 1
Definition of the chosen BSNE masts according to wind direction (U_{dir} in degrees).

Wind direction (°)	Mast
$200° < U_{dir} < 330°$	East
$330° < U_{dir} < 30°$ (clockwise)	South
$30° < U_{dir} < 50°$	South and West
$50° < U_{dir} < 150°$	West
$150° < U_{dir} < 200°$	none

speeds fulfills this condition, it was not necessary to add a zero plane displacement (Fleagle and Businger, 1980).

Finally, as a daily time-step is relevant to represent the temporal variability of the surface properties (Abdourhamane Touré et al., 2011), a daily z_0 was computed as the daily median of the 15-min z_0, but only if there were at least 3 z_0 values for the considered day.

2.3. Vegetation monitoring

Five plots of 2.0 m × 1.5 m were delimited in the field to weekly follow the barley height and cover rate using photographs and eye estimates. Barley height was measured using a meter tape. The mean maximum height of the barley tufts was measured for each plot. The barley cover rate was always estimated by the same observer on site. When barley was green, its cover rate was also estimated following Mougin et al. (2014) by a numerical treatment (CAN-EYE© software) to corroborate eye estimates. Vertical and horizontal photographs were used to check the estimates.

2.4. Saltation flux measurements

Saltation flux (F_h) is defined as the amount of sediment mass horizontally crossing a vertical section of unit length perpendicular to the wind direction integrated over the height of the saltation layer and over time. It characterizes the quantity of soil material mobilized by wind, which is not equivalent to a net budget of wind erosion over a given surface. Several authors (Ellis et al., 2009; Namikas, 2003; Panebianco et al., 2010) showed that the equations of the exponential form originally proposed by Williams (1964) (Eq. (2)) give the best representation of the vertical distribution of mass flux density, $q(z)$, from the soil surface to the average maximum saltation height.

$$q(z) = q_0 e^{-Bz} \tag{2}$$

with q_0 the value of q at $z = 0$ and B a positive empirical constant.

Consequently, saltation flux can be computed by vertically integrating the mass flux density in the saltation layer, i.e., up to 50 cm (Gillette et al., 1997), using the following equation:

$$F_h = \int_0^{0.5} q(z)dz = \frac{-q_0}{B}\left(\frac{1}{\exp(-0.5B)} - 1\right) \tag{3}$$

In the field, saltation flux was monitored on 3 masts located at the limits of the plot (West, East, and South masts; Fig. 1a). Each mast was equipped with four Big Spring Number Eight (BSNE) sand traps (Fryrear, 1986) mounted at heights of about 7, 16, 31, and 45 cm AGL, and with a large wind vane (Fig. 1b) so that the opening of all BSNE always faced the wind. The three highest BSNEs on each mast had an opening of 10 cm^2 while the lowest one had a smaller opening (2 cm^2) to get measurements close to the soil surface and to prevent the sampler from overloading as the flux is the highest there. The efficiency of the different sand-traps has been discussed thoroughly in the literature. For the BSNE sand-trap, Goossens et al. (2000) estimated the efficiency to be 100 % based on wind tunnel and field measurements. However, the efficiency may depend on the soil size distribution and the wind speed (Goossens and Buck, 2012; Mendez et al., 2011). For an aeolian sand, Shao et al. (1993) found an overall efficiency of the BSNE sand traps of 90 ± 5 % in the wind tunnel. From these results, we can consider that the efficiency of the BSNE is higher than 90 % for the Tunisian sandy soils, and in the following, the value of 100 % obtained by Goossens et al. (2000) was used to make the computations.

The mass flux density, $q(z)$ (with z the height of the center of the opening), was obtained by dividing the collected mass of sediment, $M(z)$, by the surface of the opening, $s(z)$:

$$q(z) = M(z)/s(z) \tag{4}$$

BSNEs were emptied about once a week (Appendix 1). For each measurement period, saltation flux was computed from the mast ensuring that measurements were made with the maximum fetch during erosive events, thus depending on the direction of maximum wind speeds during the considered period. When this direction was between 200° and 330°, only measurements from the East mast were considered; when it was between 330° and 30° (passing by the North (0°)), only measurements from the South mast were considered; when it was between 30° and 50°, measurements from the South and West masts were averaged; and when it was between 50° and 150°, only measurements from the West mast were considered (Table 1). Finally, if the direction of erosive winds varied too much during the measurement period and cannot be recorded with only one BSNE sand trap or the two same adjacent sand traps, then the measurements were rejected.

2.5. Computation of the dust Uplift Potential

In order to isolate the specific role of the wind from that of the surface properties in the variability of aeolian fluxes, Marsham et al. (2011) proposed to compute a diagnostic parameter, the Dust Uplift Potential (*DUP*, in $m^3\ s^{-3}$).

$$\begin{cases} DUP = U^3\left(1 + \frac{U_t}{U}\right)\left(1 - \frac{U_t^2}{U^2}\right) & when\ U > U_t \\ DUP = 0 & when\ U < U_t \end{cases} \tag{5}$$

where U_t is the threshold wind speed allowing wind erosion (in $m\ s^{-1}$), and U is the wind speed (in $m\ s^{-1}$).

The *DUP* allows to calculate the maximum wind erosion that could be produced for a given wind speed for a totally smooth erodible surface. Therefore, in Equation (5), U_t corresponds to the minimum U_t corresponding to a smooth bare surface.

When the Dar Dhaoui experimental range was totally deprived of vegetation, tilled with a disc plough and levelled with a wood board (so that its surface was as smooth as possible), Dupont et al. (2018) determined the threshold wind friction velocity $u_{*t} = 0.22\ m\ s^{-1}$. Assuming a logarithmic wind profile (Eq. (1)) and $z_0 = 5\ 10^{-4}$ m (the median z_0 computed for the period September-October 2016, i.e., just before seeding barley again – see §3.2), this corresponds to $U_t = 4.56\ m\ s^{-1}$ at 2 m. To compute the *DUP*, we used the 15-minute average wind speed U measured at 2 m AGL by the 2D sonic anemometer.

Following Bergametti et al. (2017), to determine the role played by rain in the variations measured in the wind erosion flux, a "wet" *DUP*, DUP_{wet}, was also computed: *DUP* was set to zero during rain events and during the following 12 h after the rain stops according to the recommendations of Bergametti et al. (2016) for sandy soils in the Sahel.

3. Results

3.1. Dynamics of crop vegetation

Fig. 3 presents the general view of the barley field from the beginning of barley growth (03/11/2015) to the end of the harvest (24/04/2016). On 03/11/2015, the barley was green (Fig. 3) and about 10 cm high (Fig. 4a), but the cover rate was less than 1 % (Fig. 4b). Fig. 3 (03/11/2015) shows the clods that formed consecutively to tillage on humid

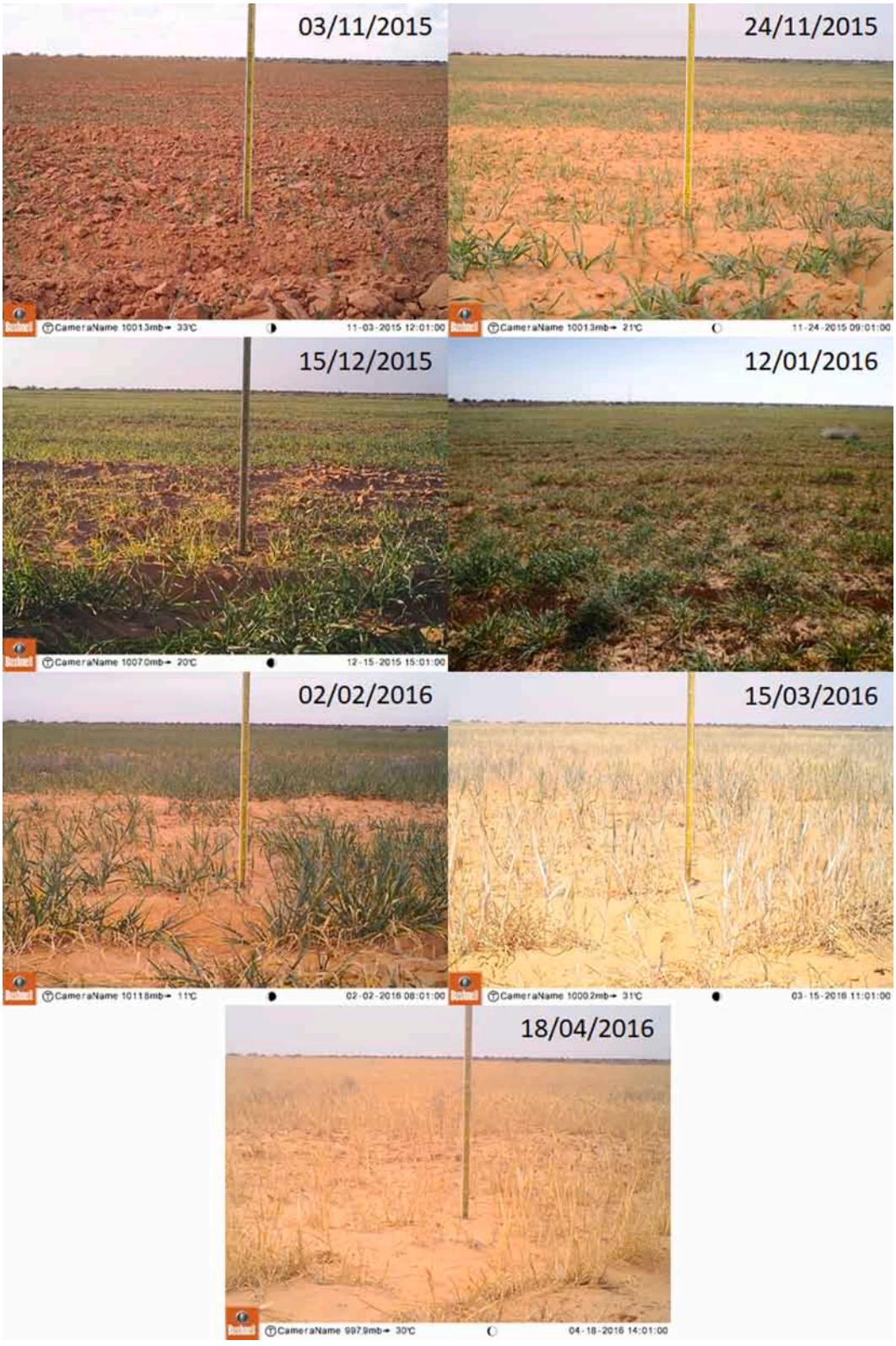

Fig. 3. General view of the barley field from the onset of barley growth (03/11/2015) to the beginning of harvest (18/04/2016).

soil. About three weeks later (24/11/2015), the barley had grown to a height of about 16 cm (Fig. 4a), but the cover rate was still about 1 % (Fig. 4b). About three weeks later (15/12/2015), the height was 20 cm (Fig. 4a) and the cover rate 14 % on average, but locally it reached 25 % (Fig. 4b). One month later (12/01/2016), stems had developed, the barley height was quite similar, around 20 cm on average (Fig. 4a), but the cover rate had considerably increased to reach 35 % in some places (Fig. 4b). The large standard deviations associated to the cover rate can be explained by the sowing density which was highly variable because of the manual sowing on the fly. On 02/02/2016, ears had developed and the barley started to turn brown (Fig. 3), but continued to grow to reach up to 30 cm height (Fig. 4a). However, the cover rate decreased to 20 %

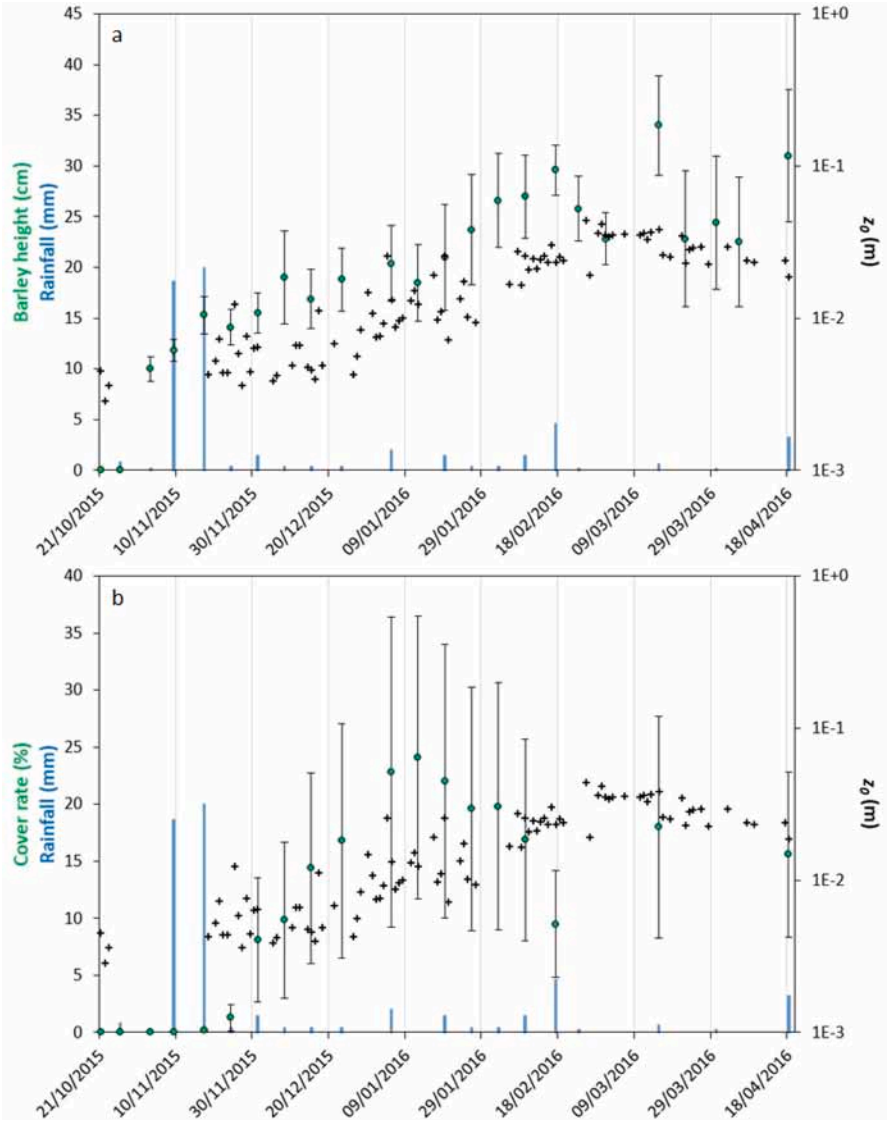

Fig. 4. Daily median of the aerodynamic roughness length (z_0 in m – black crosses; right axis) along with the temporal evolution of the (a) barley height (in cm – green dots; left axis) and (b) barley surface cover rate (in % – green dots; left axis) averaged on the 5 plots distributed in the experimental field (see §2.4) from 21/10/2015 (date of sowing) to 18/04/2016 (first day of harvest). In both cases, error bars represent the corresponding standard deviation. Rainfall (in mm) for each measurement period is also reported (blue bars). (For interpretation of the references to colour in this figure legend, the reader is referred to the web version of this article.)

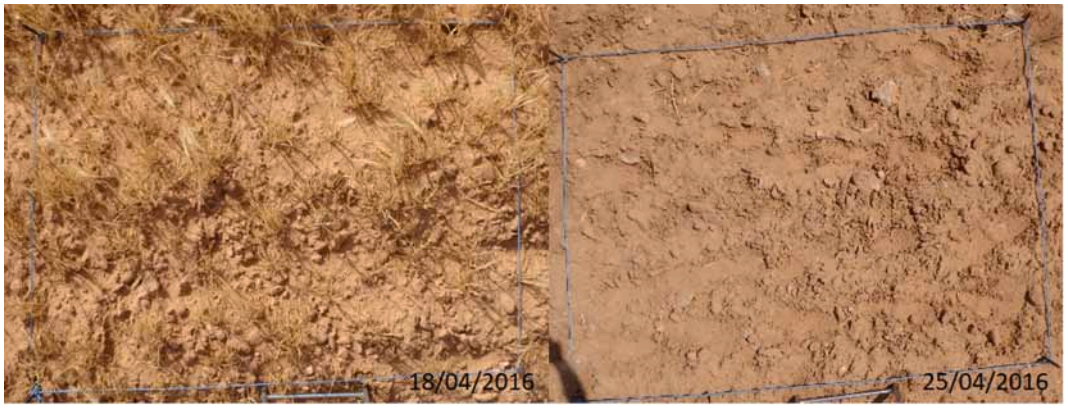

Fig. 5. Views of one of the plot in the barley field dedicated to vegetation monitoring just before (18/04/2016) and after (25/04/2016) harvest.

on average (Fig. 4b), which can be explained by the shriveling of the leaves of the browning barley. On 15/03/2016, the maximum height (34 cm on average – Fig. 4a) was reached, and the cover rate was about 20 % on average (Fig. 4b). The barley was mainly brown (Fig. 3). One month later, just before harvest (18/04/2016), barley was totally brown (Fig. 3), and its height and cover did not significantly change (Fig. 4). This period corresponds to the filling of the barley grains. Finally, Fig. 5 presents two views of one of the plots in the barley field dedicated to vegetation monitoring just before (18/04/2016) and after (25/04/2016) harvest. It shows that the harvest, which consists in removing

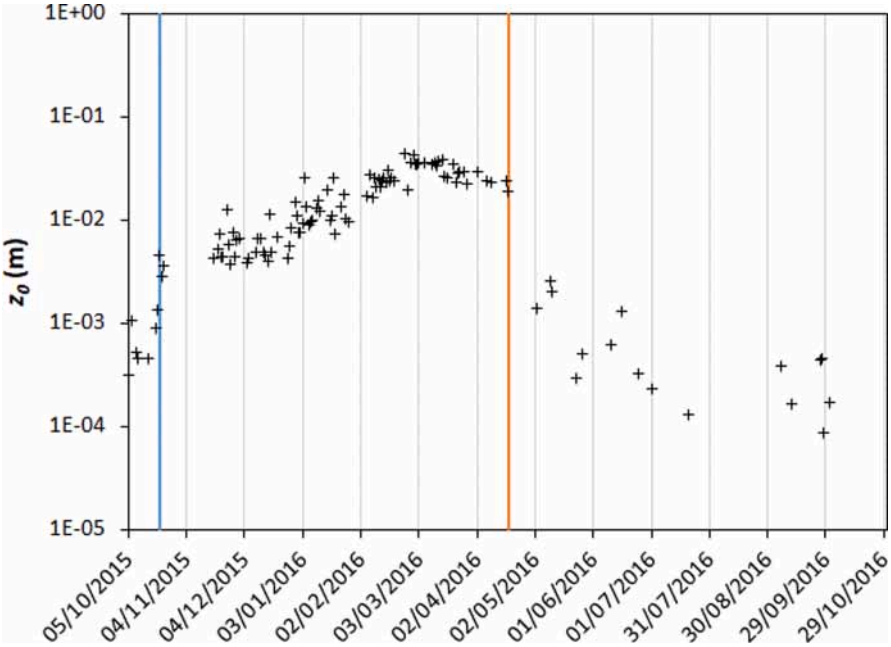

Fig. 6. Daily median of the aerodynamic roughness length (z_0 in m) from 05/10/2015 to 31/10/2016. The blue and orange vertical lines indicate the dates of the sowing (21 October 2015) and beginning of the harvest (from 18 to 22 April 2016), respectively. (For interpretation of the references to colour in this figure legend, the reader is referred to the web version of this article.)

barley tufts, collecting the whole plant from the roots to the ears, left the soil surface nearly bare (natural vegetation was not removed) and disturbed (footprints of the farmers are clearly visible on 25/04/2016 in Fig. 5).

3.2. Dynamics of z_0

The daily medians of z_0 over the study period ranged between 8.7×10^{-5} m and 4.4×10^{-2} m (Fig. 6). This order of magnitude is consistent with the values reported by Marticorena et al. (2006) for different sites in southern Tunisia and those of the literature. The maximum value compares to the roughness length of grassy surfaces and the minimum to that measured on interdunal areas of the Douz sand sea. Here, the minimum value was obtained at the end of September 2016, i.e. short before tillage, and the maximum value at the end of February 2016, i.e. when barley reached its maximum height (Fig. 4a). Because tillage was performed on a wet soil, it formed clods on the soil surface (Fig. 3 on 03/11/2015). The presence of clods led z_0 to increase from 7.1×10^{-4} m (average z_0 from 5 to 20 October 2015) before tillage to 3.7×10^{-3} m (average z_0 from 21 to 23 October 2015) after tillage. From the appearance of the stems (around 12/01/2016), z_0 followed the temporal evolution of the barley height (Fig. 4a), but not that of barley cover rate (Fig. 4b). Indeed, a significant relationship is obtained between z_0 and the barley height ($R^2 = 0.51$; N = 11 – Fig. 7a), but not between z_0 and the barley surface cover rate ($R^2 = 0.06$; N = 9 – Fig. 7b). This is in agreement with Udagawa (1966) who found, during the experiment he conducted on a barley field in the Central Agricultural Experiment Station of Kitamoto (Japan), that the seasonal change in z_0 followed more closely the change of the plant height than that of the leaf area index (which includes both the surface area of barley stems and ears). This result was corroborated by Fang and Sill (1992) who showed that, for real surfaces (such as cropland, grassland…), z_0 was proportional to the average roughness element height. After harvest, a clear drop in z_0 was observed at our study site (Fig. 6). This can be explained by the removal of the barley leaving little vegetation on the field and by the trampling of the surface (Fig. 5 on 25/04/2016). Afterwards, z_0 continued to decrease as the remaining dry vegetation was degraded because of the action of climate, ants, termites, and rodents (Jouquet et al., 2021), and as the clods were eroded by wind abrasion and rain.

3.3. Wind characteristics and dynamics of DUP

The seasonal wind roses for all the wind speeds above the threshold of 4.56 m s^{-1} (see Section 2.5) reveal a clear seasonality, with the highest wind speeds recorded mainly during springtime (Fig. 8b). This is agreement with the study performed by Khatelli and Gabriels (2000) who showed that active winds (U greater than 3 m s^{-1} at 1.5 m height) occurred mostly during winter and spring in southern Tunisia. The seasonality of the surface wind speed observed in the Dar Dhaoui plot is also consistent with the seasonality observed at the IRA Médenine using the 8-year measurements available (Appendix 2). During the field experiment, dominant directions of erosive winds were from West-South-West in winter (Fig. 8a) and conversely from the East-North-East in summer (Fig. 8c). In spring and autumn (Fig. 8b and d), most of erosive winds blew from the North even though the highest wind speeds (greater than 8 m s^{-1}) were recorded from the West-South-West.

Fig. 9 presents the temporal evolution of the *DUP* during the field campaign. 15-min *DUP* varied from 0 to 3 500 $m^3 s^{-3}$, with the maximum value occurring on 11 May 2016 (Fig. 9a). 60 % of the annual DUP is observed in spring, from March to June (Fig. 9b). In other words, spring is the period during which erosive winds are the highest and the most frequent.

3.4. Dynamics of the saltation flux

The annual saltation flux measured on the barley field was 448 kg m^{-1}. It is of the same order as the annual saltation flux measured on traditionally cultivated millet fields by different authors using the same sand traps. In western Niger, from 1996 to 1998, Rajot (2001) measured annual saltation flux of 209 to 601 kg m^{-1} and Abdourhamane Touré et al. (2011) measured annual saltation flux of 137 to 320 kg m^{-1} from 2006 to 2008. More recently, in western Niger, Abdourhamane Touré et al. (2019) measured annual saltation flux of 368 to 2902 kg m^{-1} from 2012 to 2016.

Fig. 10 presents the saltation flux measured in the field from 21/10/2015 to 11/11/2016. From 21/10/2015 to the beginning of May 2016,

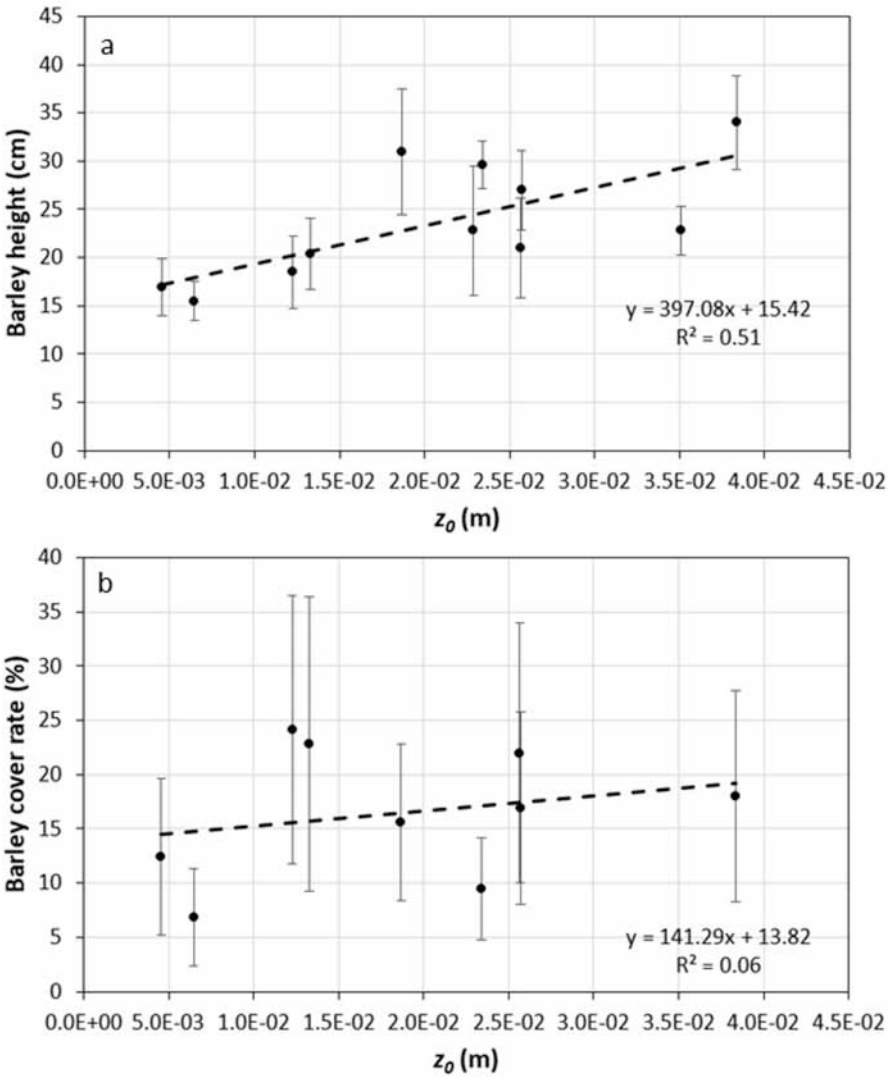

Fig. 7. Scatterplot of (a) the barley height (in cm), and (b) the barley surface cover rate (in %) as a function of the daily median of the aerodynamic roughness length (z_0 in m). In both cases, error bars represent the corresponding standard deviation. The linear regression line (dashed line) and its equation are also reported.

saltation fluxes were low with all values below 10 kg m^{-1} $period^{-1}$. After this date, larger fluxes were measured with 81 % of the wind erosion that occurred during 6 periods: 11–12 May 2016 (80.5 kg m^{-1}), 24 May-07 June 2016 (53.7 kg m^{-1}), 12–20 July 2016 (33.7 kg m^{-1}), 07–12 September 2016 (23.1 kg m^{-1}), 25 October-1 November 2016 (27.8 kg m^{-1}), and 1–11 November 2016 (144.6 kg m^{-1}). Compared to the collecting duration, the most intense period of wind erosion occurred on 11–12 May 2016 (F_h = 69.9 kg m^{-1} day^{-1}) followed by the 1–11 November 2016 (F_h = 14.5 kg m^{-1} day^{-1}), whereas F_h was about 4 kg m^{-1} day^{-1} during the four other periods.

4. Discussion

4.1. Impact of barley growth on the flux of wind-blown sand

Fig. 11 presents a comparison between the measured saltation flux and the wind erosivity (*DUP*) accumulated over the duration of the field experiment and normalized for the sake of comparison. The *DUP* from the sowing (21 October 2015) to the harvest (18 April 2016) represents about 40 % of the annual *DUP*, but the saltation fluxes measured during this period do not exceed 3 % of the annual value. The remaining 97 % of the annual saltation flux are recorded from 11 May to 11 November 2016. In fact, the wind erosivity as indicated by the *DUP* increased rather constantly from the beginning of January 2016 to the end of the experiment, whereas wind erosion was mainly measured from the beginning of May 2016. This clearly states that wind speed is not the main driver of the seasonality of wind erosion on the barley field in this region.

This observation is reinforced by the comparison of the temporal evolutions of the aerodynamic roughness length and saltation flux (Fig. 12). During the growth of the barley, z_0 increased and the saltation flux remained almost nil; then, after the harvest, z_0 decreased dramatically (by about one order of magnitude) while the cumulated saltation flux increased. Clearly, the difference observed between the temporal evolutions of the *DUP* and that of the saltation flux is due to the presence/absence of vegetation as the barley's height drives the evolution of z_0 (Fig. 7a).

A quantitative assessment of how much wind erosion has been reduced during the barley's growth cannot be precisely done because this would have required that a reference surface not cultivated was instrumented in parallel. However, an attempt can be done assuming that the sediment flux is proportional to the *DUP*: if we consider the post-harvest period as a reference for a non-cultivated surface and the same efficiency during the barley growth as during the post-harvest, comparing the sediment flux obtained for a same value of *DUP* during the two periods would allow to estimate how much wind erosion has

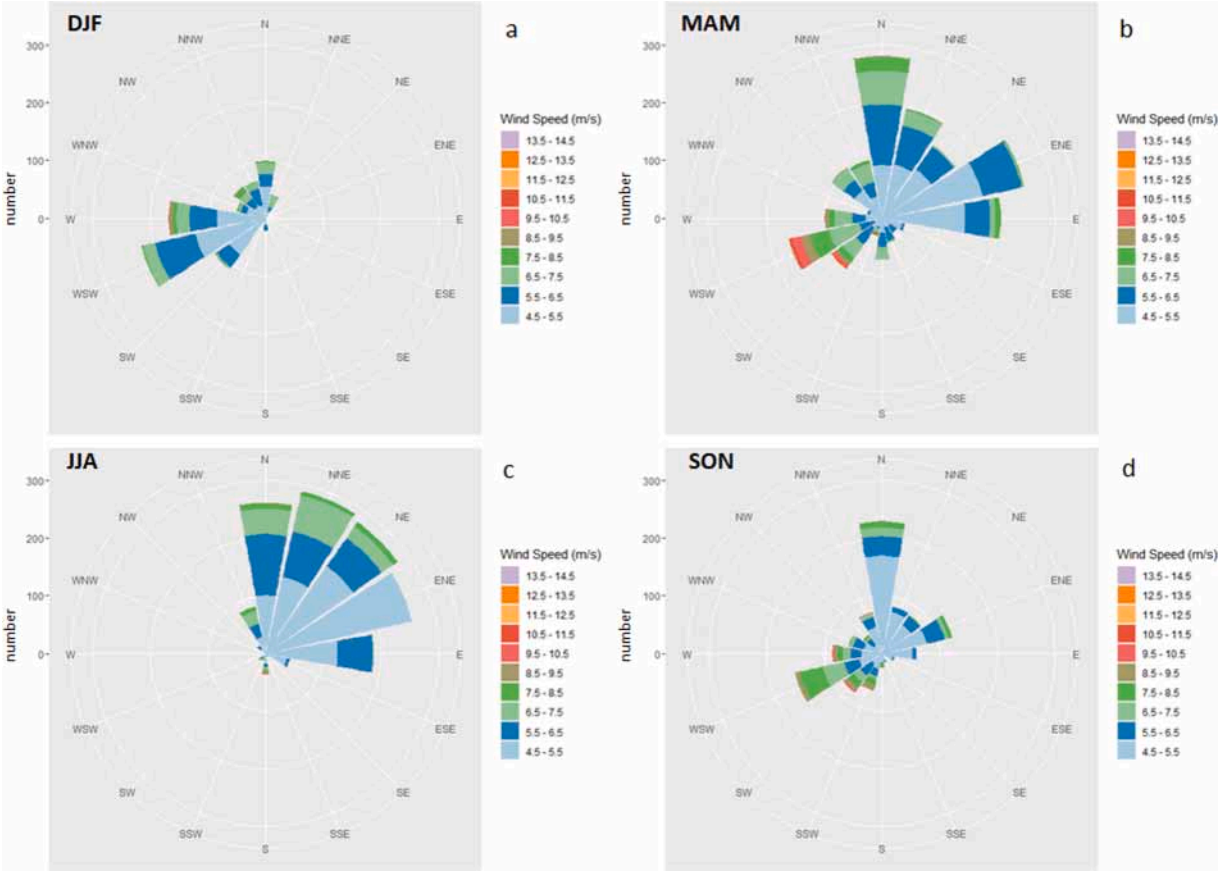

Fig. 8. The wind roses of the 15-min wind data measured from 21/10/2015 to 11/11/2016 at 2 m AGL with a 2D sonic anemometer. Only the wind speeds above the threshold of 4.56 m s^{-1} are considered (see Section 2.5) and the four seasons are distinguished: winter (DJF - a), spring (MAM - b), summer (JJA - c), and autumn (SON - d).

been reduced during barley growth. In Table 2, we present a comparison for 2 periods during which *DUP* was of the same order of magnitude before and after harvest. For both selected periods, before harvest, barley height and surface cover were close to 20 cm and 20 %, respectively, and z_0 was around 10^{-2} m, and after harvest, z_0 drops to ~ 1 10^{-4} m.

In case #1, a reduction of about a factor 16 is observed whereas in case #2, the reduction is of a factor 100. This computation provides an estimate of how the barley's growth has reduced wind erosion, and shows that this reduction is not linear.

4.2. Impact of precipitation on the flux of wind-blown sand

The direct effect of precipitation (i.e., excluding that on the vegetation growth) can be estimated by comparing the *DUP* computed when accounting, or not, for the inhibition of wind erosion by precipitation. For the experimental period, the accumulated *DUP* and DUP_{wet} were 828 281 $m^3 s^{-3}$ and 649 657 $m^3 s^{-3}$, respectively. This indicates that for a period covering more than one year and an annual rainfall of 77.6 mm, precipitation can potentially decrease wind erosion by up to 20 %. This suggests that at the scale of the year rain has a lesser direct impact on the modulation of the saltation flux than vegetation.

The impact of precipitation can be examined at a shorter time scale. From 21 October 2015 to 11 November 2016, 15 precipitation events occurred, and represented 74.0 mm of rainfall (Table 3). Depending on the period considered, the ratio between DUP_{wet} and *DUP* varied from 1 (i.e., there was no impact of rain) to 0.40 (i.e., rain inhibited wind erosion by more than a factor 2). This means that, at the scale of the event, rain may have a large impact on wind erosion, and should not be neglected when evaluating wind erosion. Otherwise, wind erosion would be overestimated. It seems that no systematic link exists between the rainfall accumulated in a sampling period and either the reduction of the *DUP*, the maximum wind speed recorded, or the frequency of exceedance of U_t by wind speed. This can be illustrated by the comparison of periods 2 and 3 during which the accumulated rainfall and maximum wind speed are of the same order of magnitude (18.6 mm and 20.0 mm for rainfall, and 7.6 m s^{-1} and 7.7 m s^{-1} for wind speed, respectively). The percentage of time U exceeded U_t was also equal (1 %). However, the DUP_{wet}/DUP ratio varied from 0.98 to 0.54. This difference can be explained by the time when precipitation and erosive winds occurred. Indeed (Fig. 13), during period 2, precipitation started at 21:20 LT on 07/11/2015 after U exceeded U_t (from 08:45 LT to 12:45 LT on 07/11/2015), whereas during period 3 precipitation started at 02:05 LT on 14/11/2015 just before U exceeded U_t (from 08:30 LT to 16:30 LT on 14/11/2015). This in-situ result supports those of the modelling study by Okin (2022) who highlighted that rain can suppress dust emission from drylands by wetting the soil surface, but only if the emissive winds occur while the soil is wet.

4.3. Impact of agricultural practices on flux of wind-blown sand

Today, Tunisian farmers use disc ploughs to till barley fields instead of the moldboard plough that was traditionally used before (Akrimi et al., 1993). As compared to the moldboard plough, disc plough was shown to increase wind erosion dramatically: on sandy soils, this increase can reach one order of magnitude (Labiadh et al., 2013). In the present case, ploughing is done simultaneously with the sowing when the soil surface is wet to allow a good start of the plant growth, but this creates clods (Fig. 3 on 03/11/2015). Several authors showed that clods play an important role in the control of wind erosion (Fryrear, 1984;

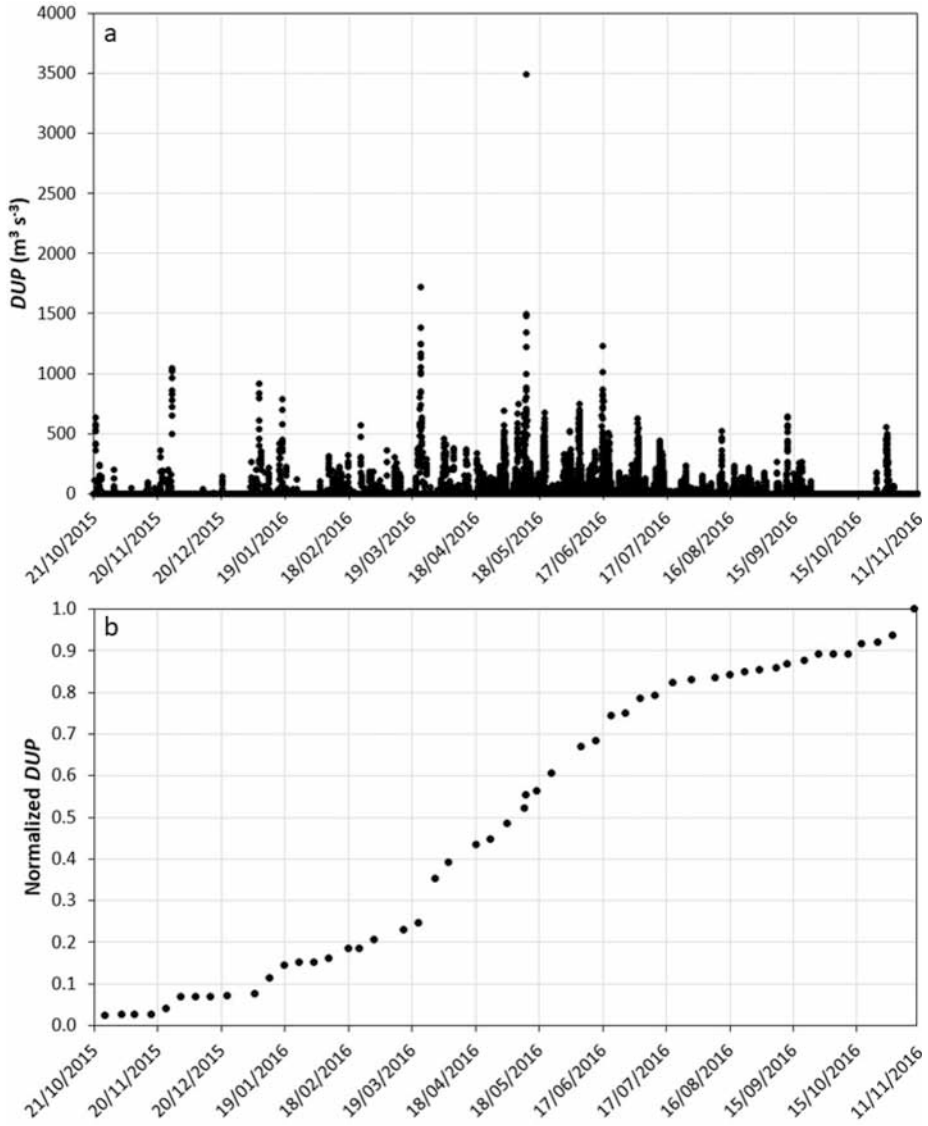

Fig. 9. Temporal evolution of (a) 15-min *DUP*, and (b) accumulative frequency of normalized *DUP* from 21/10/2015 to 11/11/2016.

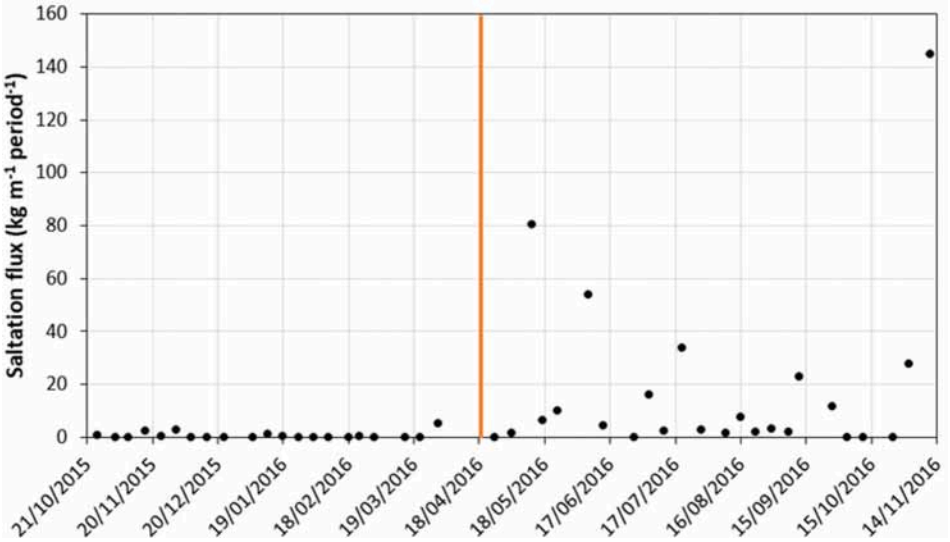

Fig. 10. Saltation flux (in kg m^{-1} $period^{-1}$) from 21/10/2015 to 11/11/2016. The orange vertical line indicates the beginning of the harvest (from 18 to 22 April 2016). (For interpretation of the references to colour in this figure legend, the reader is referred to the web version of this article.)

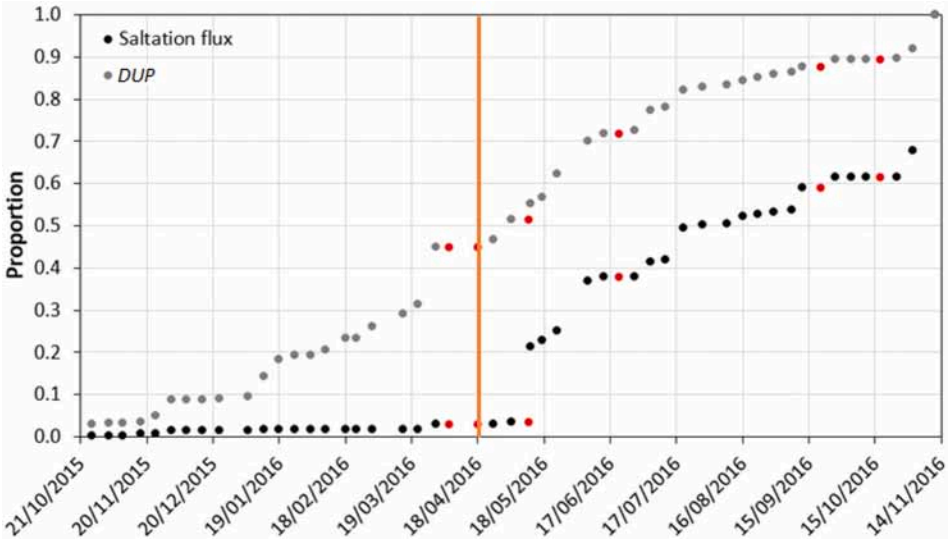

Fig. 11. Normalized saltation flux (black dots) and *DUP* (grey dots) accumulated from 21/10/2015 to 11/11/2016. Red dots correspond to the cases for which none of the three masts was retained following the analysis of wind direction. The orange vertical line corresponds to the beginning of the harvest (from 18 to 22 April 2016). (For interpretation of the references to colour in this figure legend, the reader is referred to the web version of this article.)

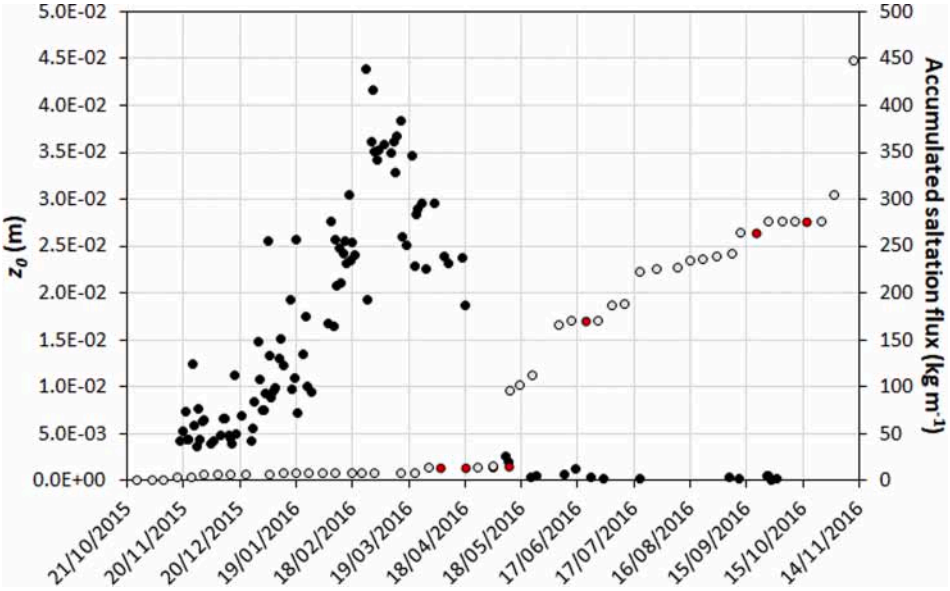

Fig. 12. Temporal evolution of z_0 (in m – black dots; left scale) and accumulated saltation flux (in kg m^{-1} – open circles; right scale) from 21/10/2015 to 11/11/2016. Red dots correspond to the cases for which none of the three masts was retained following the analysis of wind direction.

Table 2
Measured saltation flux (in kg m^{-1} day^{-1}), *DUP* (in m^3 s^{-3}), and z_0 (in m) for 2 sets of selected periods before and after harvest.

		Sampling start	Sampling end	Duration (days)	Measured saltation flux (kg m^{-1} day^{-1})	*DUP* cumulated on the period (m^3 s^{-3})	z_0 (m)
#1	Before harvest	05/01/2016	12/01/2016	7	0.14	30 893	$1.33\ 10^{-2}$
	After harvest	28/06/2016	05/07/2016	7	2.32	30 238	$\sim 3\ 10^{-4}$
#2	Before harvest	19/01/2016	26/01/2016	7	0.01	6 374	$2.57\ 10^{-2}$
	After harvest	09/08/2016	16/08/2016	7	1.06	5 984	$\sim 1\ 10^{-4}$

Zhang et al., 2004). Moreover, winds are not very strong during this period (Fig. 8d). All this concurs to limit wind erosion at the beginning of the agricultural season, i.e., in a period during which the surface deprived of vegetation should be highly susceptible to wind erosion.

When winds are the strongest (mostly in spring – Fig. 8b), barley is close to having its maximum height (about 20 cm), which protects the field's surface from wind erosion. In the present case, the sowing date which is driven by rainfall permits to minimize wind erosion in the barley field. However, this temporal coincidence favoring the reduction of wind erosion by cropped vegetation may not be systematic even in southern Tunisia: if rain occurs later in autumn, barley will also be sown later and wind erosion could occur in the field because the barley height will be too low to protect efficiently the soil surface.

In other regions of the world, the non-coincidence between the

Table 3
Accumulated rainfall (in mm) and saltation flux (in kg m^{-1} $period^{-1}$) measured for each sampling period during which precipitation occurred, and corresponding maximum wind speed (in m s^{-1}), percentage of $U > U_t$, computed *DUP* (in m^3 s^{-3}), DUP_{wet} (in m^3 s^{-3}), and DUP/DUP_{wet}.

Period	Sampling start	Sampling end	Duration (days)	Accumulated rainfall (mm)	Measured saltation flux (kg m^{-1} $period^{-1}$)	Maximum wind speed (m s^{-1})	Percentage of $U > U_t$	*DUP* (m^3 s^{-3})	DUP_{wet} (m^3 s^{-3})	DUP_{wet}/ *DUP*
1	21/10/ 2015	26/10/ 2015	5	0.8	0.94	10.2	7 %	19,560	19,077	0.98
2	03/11/ 2015	09/11/ 2015	6	18.6	0.00	7.6	1 %	461	452	0.98
3	09/11/ 2015	17/11/ 2015	8	20.0	2.24	7.7	1 %	1 153	627	0.54
4	24/11/ 2015	01/12/ 2015	7	1.4	2.78	6.7	5 %	24 505	24 505	1.00
5	23/12/ 2015	05/01/ 2016	13	2.0	0.06	6.0	2 %	4 421	4 421	1.00
6	12/01/ 2016	19/01/ 2016	7	1.4	0.24	10.5	7 %	25 048	20 657	0.82
7	02/02/ 2016	09/02/ 2016	7	1.4	0.03	11.8	4 %	8 109	4 653	0.57
8	09/02/ 2016	18/02/ 2016	9	4.6	0.00	9.4	7 %	19 076	18 608	0.98
9	01/03/ 2016	15/03/ 2015	14	0.6	0.17	9.4	4 %	19 593	18 411	0.94
10	05/04/ 2016	18/04/ 2016	13	3.2	NA	12.5	7 %	34 188	26 659	0.78
11	03/05/ 2016	11/05/ 2016	8	1.4	NA	13.8	7 %	30 723	20 835	0.68
12	11/05/ 2016	12/05/ 2016	1	3.8	80.6	26.8	19 %	25 450	10 257	0.40
13	12/09/ 2016	20/09/ 2016	8	3.6	NA	14.4	5 %	8 267	7 969	0.96
14	20/09/ 2016	27/09/ 2016	7	6.6	2.84	8.9	6 %	10 625	9 156	0.86
15	27/09/ 2016	04/10/ 2016	7	4.6	1.41	8.6	1 %	333	165	0.49

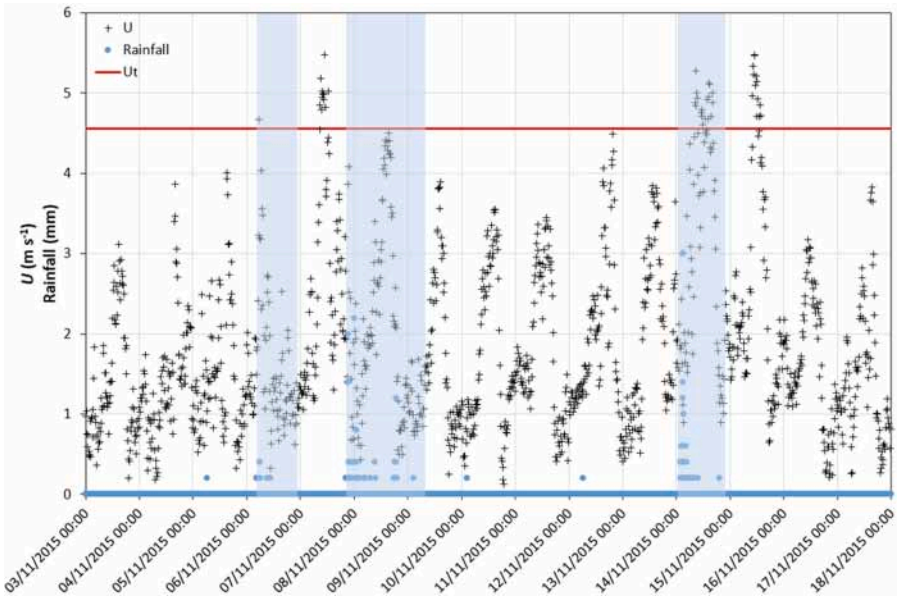

Fig. 13. 15-min wind speed (U in m s^{-1} – black crosses) and 5-min rainfall (in mm – blue circles) measured from 3 to 17 November 2015. Horizontal red line recalls the value of the wind erosion threshold used to compute the *DUP* (U_t = 4.56 m s^{-1} at 2 m). Light blue rectangles delimit the time during which wind erosion was inhibited because of precipitation in the computation of the *DUP*. (For interpretation of the references to colour in this figure legend, the reader is referred to the web version of this article.)

occurrence of high winds and vegetation development may favor wind erosion. For example, in Niger, Rajot (2001) and Abdourhamane Touré et al. (2011) showed that wind erosion on fields cultivated with pearl millet reached its maximum in May and June, at the beginning of the wet season. This corresponds to the time of the year when the soil surface is almost bare because crop residues from the previous rainy season have disappeared and the pearl millet has not started to grow, and also to the period when the *DUP* is the highest (Bergametti et al., 2020). In eastern Niger, the *DUP* can be as high in the dry season as in the wet one so that wind erosion can also occur in the dry season (Abdourhamane Touré et al., 2019). Our results suggest that in any semi-arid region, the seasonal dynamic of wind erosion is driven by the temporal phasing between the occurrence of high wind speeds and the dynamics of vegetation that depends on the precipitation regime.

97 % of wind erosion fluxes were measured between mid-May and mid-November 2016, i.e., when soil surface was almost bare because farmers collected both barley seeds and straws, which leaves the soil surface nearly bare after harvest. This result highlights the importance of considering the entire crop cycle over a full climatic year to truly assess the impact of agricultural practices. Abdourhamane Touré et al.

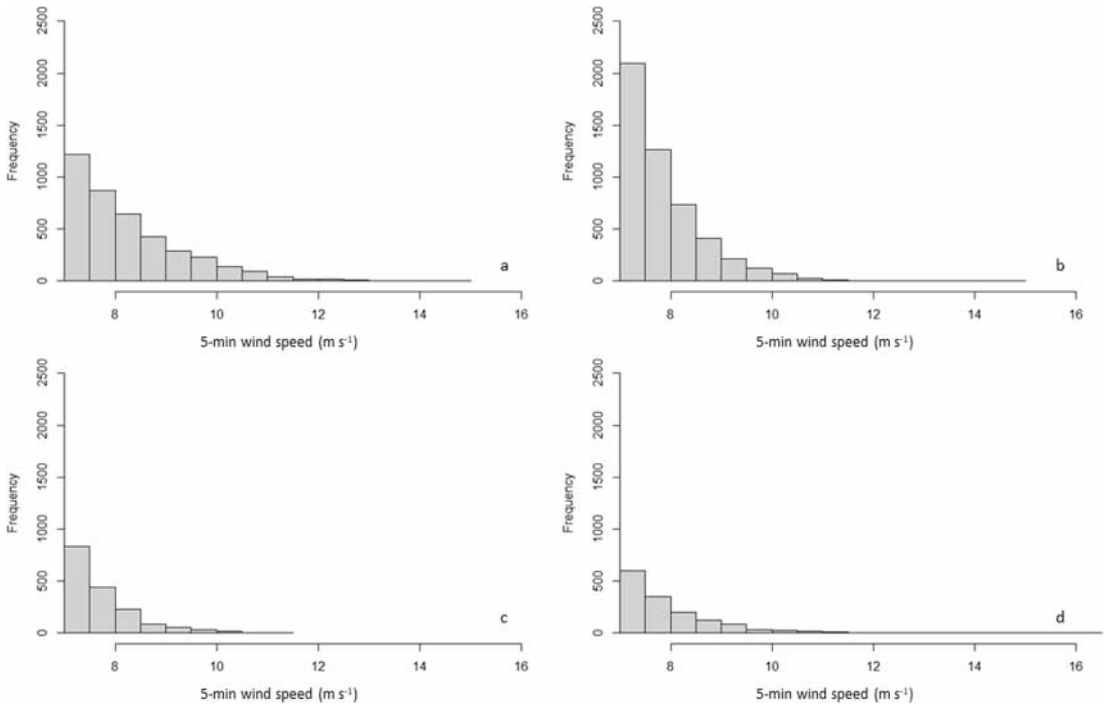

Fig. A2. Histogram of the 5-min wind speed (in m s^{-1}) above 7 m s^{-1} measured at the meteorological station installed in El Fjé from 09/02/2014 to 31/12/2021 during (a) wintertime, (b) springtime, (c) summertime, and (d) autumn.

(2011) showed that a minimal cover rate of about 2 % (100 kg ha^{-1}) is sufficient to reduce wind erosion in pearl millet fields in the Sahel. Similarly, Vos et al. (2022) emphasized the strong relationship existing between soil cover and saltation flux in croplands of South Africa, and recommended to maintain stubbles in the field to minimize wind erosion. Also, Pi et al. (2020) showed that standing crop residues can provide a significant protection to the soil surface from wind erosion. In order to reduce the impact of wind erosion on croplands, Tunisian farmers should consider leaving straws in the field after harvest instead of collecting them. Of course, the benefit of this practice regarding wind erosion must be balanced against the necessity of the farmers to feed the livestock.

5. Conclusions

Wind erosion and its drivers (meteorology and surface characteristics) were monitored in a traditionally cultivated barley field in southern Tunisia during agricultural year 2015–2016. The aim of the experiment was to disentangle the respective roles of meteorology, surface properties, and human practices on wind erosion.

97 % of wind erosion fluxes were measured between mid-May and mid-November 2016. Tillage of the field was performed at the same time as the sowing and when the soil was sufficiently wet to allow a good start of barley's growth. Tillage creates clods, which protects the soil surface from wind erosion in a period when winds are not very strong. All this limits wind erosion before the vegetation has started to grow. Barley reaches intermediate heights and cover rates between February and April, which is known to be the period of strongest winds in southern Tunisia. This produces a roughness of the order of cm and the surface is then well protected from wind erosion by the vegetation. So, traditional practices to produce barley (date of tillage and sowing) allow to limit wind erosion. The only way to improve this strategy and further limit wind erosion would probably consist in maintaining a minimum coverage of the surface in the post-harvest period, in particular by leaving some of the vegetation residues on the surface (see for instance Abdourhamane Touré et al. (2011) or Pi et al. (2020)). In the use of these vegetation residues, it will then be a matter of finding the best balance between soil cover and feed for the herds.

More generally, this study demonstrates the importance to account for the seasonality of both wind and vegetation together with human practices when studying wind erosion. On the one hand, this may help defining optimal land management to fight wind erosion and limit its consequences on the environment. On the other hand, neglecting one of these parameters (wind, vegetation, human practices) may induce a net overestimation/underestimation of the phenomenon in model estimates. Consequently, methodologies such as the one developed by Stanelle et al. (2014) to estimate dust emission fluxes from croplands, i.e., which prevents dust emission when topsoil is wet and during the growing season of crops and increases the wind erosion threshold to account for tillage, must be encouraged but also improved (as an example, the wind erosion threshold can be increased or decreased according to the tillage technique).

Declaration of Competing Interest

The authors declare that they have no known competing financial interests or personal relationships that could have appeared to influence the work reported in this paper.

Data availability

The data used in this manuscript (Rajot et al., 2022) are available for download for research and educational purposes in DataSuds at https://doi.org/10.23708/URXJ25.

Acknowledgements

The authors would like to thank: (i) Houcine Khatteli, Director of the Institut des Régions Arides (IRA) of Médenine, for the constant support of IRA in all research related to wind erosion, and in particular for giving us access to the Dar Dhaoui's experimental range and for the IRA's logistic help during the whole experiment to ensure the success of the campaign, (ii) the watchmen of the experimental station (Noureddine Boukhli, Mokhtar Elghoul and Mousbah Elghoul) for their constant help

and surveillance of the experimental system, and (iii) Prof. Stéphane Alfaro for his patience in revising the paper. Wind roses (Fig. 8) were made adapting the R program by Andy Clifton.

Appendix A. Dates of beginning and end of saltation measurement periods

Beginning date	End date
21/10/2015*	26/10/2015
26/10/2015	03/11/2015
03/11/2015	09/11/2015
09/11/2015	17/11/2015
17/11/2015	24/11/2015
24/11/2015	01/12/2015
01/12/2015	08/12/2015
08/12/2015	15/12/2015
15/12/2015	23/12/2015
23/12/2015	05/01/2016
05/01/2016	12/01/2016
12/01/2016	19/01/2016
19/01/2016	26/01/2016
26/01/2016	02/02/2016
02/02/2016	09/02/2016
09/02/2016	18/02/2016
18/02/2016	23/02/2016
23/02/2016	01/03/2016
01/03/2016	15/03/2016
15/03/2016	22/03/2016
22/03/2016	30/03/2016
30/03/2016	05/04/2016
05/04/2016	18/04/2016
18/04/2016	25/04/2016
25/04/2016	03/05/2016
03/05/2016	11/05/2016
11/05/2016	12/05/2016
12/05/2016	17/05/2016
17/05/2016	24/05/2016
24/05/2016	07/06/2016
07/06/2016	14/06/2016
14/06/2016	21/06/2016
21/06/2016	28/06/2016
28/06/2016	05/07/2016
05/07/2016	12/07/2016
12/07/2016	20/07/2016
20/07/2016	29/07/2016
29/07/2016	09/08/2016
09/08/2016	16/08/2016
16/08/2016	23/08/2016
23/08/2016	30/08/2016
30/08/2016	07/09/2016
07/09/2016	12/09/2016
12/09/2016	20/09/2016
20/09/2016	27/09/2016
27/09/2016	04/10/2016
04/10/2016	11/10/2016
11/10/2016	17/10/2016
17/10/2016	25/10/2016
25/10/2016	01/11/2016
01/11/2016	11/11/2016

*BSNEs were installed on 21/10/2015 on the East mast, and on 22/10/2015 on the West and South masts.

Appendix B. Seasonality of surface wind speed in the Jeffara plain

In February 2014, a ground-based station dedicated to the monitoring of dust episodes was installed in the campus of the Institut des Régions Arides (IRA) of Médenine in El Fjé (see Bouet et al. (2019) for a detailed description). Among the instruments deployed at the station, a meteorological station identical to the one used in Dar Dhaoui during the field experiment measures wind speed (average and maximum), air temperature, relative humidity, and rainfall at a 5-min time step. Data is freely distributed via the INDAAF (International Network to study Deposition and Atmospheric composition in Africa) database (https://indaaf.obs-mip.fr/catalogue/) at a one-hour time step.

Fig. A2 presents a histogram of the 5-min wind speed (in m s^{-1}) above 7 m s^{-1}, a common threshold wind speed used in many studies (Marsham et al., 2011; Okin, 2022), measured at the meteorological station installed in El Fjé according to the season. It can be seen that high wind speeds are more frequently observed in spring (Fig. A2b), and in winter (Fig. A2a) even though the highest wind speed is recorded in autumn (U_{max} = 16.3 m s^{-1} in autumn *vs* U_{max} = 14.7 m s^{-1} in winter and spring).

References

Abdourhamane Touré, A., Rajot, J.L., Garba, Z., Marticorena, B., Petit, C., Sebag, D., 2011. Impact of very low crop residues cover on wind erosion in the Sahel. Catena 85, 205–214. https://doi.org/10.1016/j.catena.2011.01.002.

Abdourhamane Touré, A., Tidjani, A.D., Rajot, J.L., Marticorena, B., Bergametti, G., Bouet, C., Ambouta, K.J.M., Garba, Z., 2019. Dynamics of wind erosion and impact of vegetation cover and land use in the Sahel: A case study on sandy dunes in southeastern Niger. Catena 177, 272–285. https://doi.org/10.1016/j.catena.2019.02.011.

Akrimi, N., Kardous, M., Taamallah, H., 1993. Mouvements de sable en relation avec la nature et la vitesse de certains outils de travail du sol en zones arides (étude d'un cas pratique). Revue des Régions Arides 5, 35–57.

Bagnold, R.A., 1941. The physics of blown sand and desert dunes. Methuen, London.

Bergametti, G., Rajot, J.L., Pierre, C., Bouet, C., Marticorena, B., 2016. How long does precipitation inhibit wind erosion in the Sahel? Geophys. Res. Lett. 43 https://doi.org/10.1002/2016GL069324.

Bergametti, G., Marticorena, B., Rajot, J.L., Chatenet, B., Féron, A., Gaimoz, C., Siour, G., Coulibaly, M., Koné, I., Maman, A., Zakou, A., 2017. Dust Uplift Potential in the Central Sahel: An analysis based on 10 years of meteorological measurements at high temporal resolution. J. Geophys. Res. Atmos. 122, 12433–12448. https://doi.org/10.1002/2017JD027471.

Bergametti, G., Marticorena, B., Rajot, J.L., Siour, G., Féron, A., Gaimoz, C., Coman, A., Chatenet, B., Coulibaly, M., Maman, A., Koné, I., Zakou, A., 2020. The respective roles of wind speed and green vegetation in controlling Sahelian dust emission during the wet season. e2020GL089761 Geophys. Res. Lett. 47. https://doi.org/10.1029/2020GL089761.

Bouet, C., Labiadh, M.T., Rajot, J.L., Bergametti, G., Marticorena, B., Henry des Tureaux, T., Ltifi, M., Sekrafi, S., Féron, A., 2019. Impact of desert dust on air quality: What is the meaningfulness of daily PM standards in regions close to the sources? The example of southern Tunisia. Atmosphere 10, 452. https://doi.org/10.3390/atmos10080452.

Ceccarelli, S., Grando, S., Bailey, E., Amri, A., El-Felah, M., Nassif, F., Rezgui, S., Yahyaoui, A., 2001. Farmer participation in barley breeding in Syria, Morocco and Tunisia. Euphytica 122, 521–536. https://doi.org/10.1023/A:1017570702689.

Chi, W., Zhao, Y., Kuang, W., He, H., 2019. Impacts of anthropogenic land use/cover changes on soil wind erosion in China. Sci. Total Environ. 668, 204–215. https://doi.org/10.1016/j.scitotenv.2019.03.015.

Dupont, S., Rajot, J.-L., Labiadh, M., Bergametti, G., Alfaro, S.C., Bouet, C., Fernandes, R., Khalfallah, B., Lamaud, E., Marticorena, B., Bonnefond, J.-M., Chevaillier, S., Garrigou, D., Henry-des-Tureaux, T., Sekrafi, S., Zapf, P., 2018. Aerodynamic parameters over an eroding bare surface: Reconciliation of the Law of the Wall and Eddy Covariance determinations. J. Geophys. Res. Atmos. 123, 4490–4508. https://doi.org/10.1029/2017JD027984.

Dupont, S., Rajot, J.-L., Labiadh, M., Bergametti, G., Lamaud, E., Irvine, M.R., Alfaro, S. C., Bouet, C., Fernandes, R., Khalfallah, B., Marticorena, B., Bonnefond, J.M., Chevaillier, S., Garrigou, D., Henry-des-Tureaux, T., Sekrafi, S., Zapf, P., 2019. Dissimilarity between dust, heat, and momentum turbulent transports during aeolian soil erosion. J. Geophys. Res. Atmos. 124, 1064–1089. https://doi.org/10.1029/2018JD029048.

Ellis, J.T., Li, B., Farrell, E.J., Sherman, D.J., 2009. Protocols for characterizing aeolian mass-flux profiles. Aeolian Res. 1, 19–26. https://doi.org/10.1016/j.aeolia.2009.02.001.

Fang, C., Sill, B.L., 1992. Aerodynamic roughness length: Correlation with roughness elements. J. Wind Eng. Ind. Aerod. 41, 449–460. https://doi.org/10.1016/0167-6105(92)90444-F.

Fleagle, R.G., Businger, J.A., 1980. An introduction to atmospheric physics. Int. Geophys. Series, second ed. Academic Press, New York.

Fryrear, D.W., 1984. Soil ridge-clods and wind erosion. T. ASAE 27, 445–448.

Fryrear, D.W., 1986. A field dust sampler. J. Soil Water Conserv. 41, 117–120.

Gholizadeh, H., Zoghipour, M.H., Torshizi, M., Nazari, M.R., Moradkhani, N., 2021. Gone with the wind: Impact of soil-dust storms on farm income. Ecol. Econ. 188, 107133 https://doi.org/10.1016/j.ecolecon.2021.107133.

Gillette, D.A., Fryrear, D.W., Xiao, J.B., Stockton, P., Ono, D., Helm, P.J., Gill, T.E., Ley, T., 1997. Large-scale variability of wind erosion mass flux rates at Owens Lake 1. Vertical profiles of horizontal mass fluxes of wind-eroded particles with diameter greater than 50 μm. J. Geophys. Res. 102, 25977–25987.

Ginoux, P., Prospero, J.M., Gill, T.E., Hsu, N.C., Zhao, M., 2012. Global-scale attribution of anthropogenic and natural dust sources and their emission rates based on MODIS Deep Blue aerosol products. Rev. Geophys. 50, 36. https://doi.org/10.1029/2012RG000388.

Goossens, D., Buck, B.J., 2012. Can BSNE (Big Spring Number Eight) samplers be used to measure PM10, respirable dust, PM2.5 and PM1.0? Aeolian Res. 5, 43–49.

Goossens, D., Offer, Z., London, G., 2000. Wind tunnel and field calibration of five aeolian sand traps. Geomorphology 35, 233–252.

Greeley, R., Iversen, J.D., 1985. Wind as a geological process on Earth, Mars, Venus and Titan, Cambridge University Press. ed, Cambridge Planetary Science Series. Cambridge - London - New York - New Rochelle - Melbourne - Sydney.

Houyou, Z., Bielders, C.L., Benhorma, H.A., Dellal, A., Boutemdjet, A., 2016. Evidence of strong land degradation by wind erosion as a result of rainfed cropping in the Algerian steppe: A case study at Laghouat. Land Degrad. Develop. 27, 1788–1796. https://doi.org/10.1002/ldr.2295.

Jouquet, P., Henry-des-Tureaux, T., Bouet, C., Labiadh, M., Caquineau, S., Aroui Boukbida, H., Garcia Ibarra, F., Hervé, V., Bultelle, A., Podwojewski, P., 2021. Bioturbation and soil resistance to wind erosion in Southern Tunisia. Geoderma 403, 115198. https://doi.org/10.1016/j.geoderma.2021.115198.

Kallel, M.R., 2001. Hydrologie de la Jeffara Tunisienne. Rapport interne, DG-RE, Tunis, p. 65.

Kardous, M., 2005. Quantification de l'érosion éolienne dans les zones arides tunisiennes : approche expérimentale et modélisation (Doctorat). Université Paris XII Val de Marne, Créteil.

Khalfallah, B., Bouet, C., Labiadh, M.T., Alfaro, S.C., Bergametti, G., Marticorena, B., Lafon, S., Chevaillier, S., Féron, A., Hease, P., Henry des Tureaux, T., Sekrafi, S., Zapf, P., Rajot, J.L., 2020. Influence of atmospheric stability on the size distribution of the vertical dust flux measured in eroding conditions over a flat bare sandy field. J. Geophys. Res. Atmos. 125, e2019JD031185 https://doi.org/10.1029/2019JD031185.

Khatelli, H., 1996. Erosion éolienne en Tunisie aride et désertique, analyse des processus et recherches des moyens de lutte (Thèse de Doctorat en Sciences Biologiques Appliquées). Université de Gent.

Khatelli, H., Gabriels, D., 2000. Effect of wind direction on aeolian sand transport in southern Tunisia. Int. Agrophysics 14, 291–296.

Khatelli, H., 1981. Recherches stationnelles sur la désertification dans la Djeffara (Tunisie). Dynamique de l'érosion éolienne (Thèse de 3ème cycle). Université Paris I (Panthéon - Sorbonne).

Labiadh, M., Bergametti, G., Attoui, B., Sekrafi, S., 2011. Particle size distributions of South Tunisian soils erodible by wind. Geodin. Acta 24, 39–49.

Labiadh, M., Bergametti, G., Kardous, M., Perrier, S., Grand, N., Attoui, B., Sekrafi, S., Marticorena, B., 2013. Soil erosion by wind over tilled surfaces in South Tunisia. Geoderma 202–203, 8–17. https://doi.org/10.1016/j.geoderma.2013.03.007.

Larney, F.J., Bullock, M.S., Janzen, H.H., Ellert, B.H., Oslon, E.C.S., 1998. Wind erosion effects on nutrient redistribution and soil productivity. J. Soil Water Conserv. 53, 133–140.

Lee, J.A., Wigner, K.A., Gregory, J.M., 1993. Drought, wind and blowing dust on the southern High Plains of the United States. Phys. Geogr. 14, 56–67. https://doi.org/10.1080/02723646.1993.10642467.

Mahowald, N.M., Rivera Rivera, G.D., Luo, C., 2004. Comment on "Relative importance of climate and land use in determining present and future global soil dust emission" by I. Tegen et al. Geophys. Res. Lett. 31, L24105. https://doi.org/10.1029/2004GL021272.

Marsham, J.H., Knippertz, P., Dixon, N.S., Parker, D.J., Lister, G.M.S., 2011. The importance of the representation of deep convection for modeled dust-generating winds over West Africa during summer. Geophys. Res. Lett. 38, L16803. https://doi.org/10.1029/2011GL048368.

Marticorena, B., Kardous, M., Bergametti, G., Callot, Y., Chazette, P., Khatteli, H., Le Hégarat-Mascle, S., Maillé, M., Rajot, J.-L., Vidal-Madjar, D., Zribi, M., 2006. Surface and aerodynamic roughness in arid and semiarid areas and their relation to radar backscatter coefficient. J. Geophys. Res. 111, F03017. https://doi.org/10.1029/2006JF000462.

Mendez, M.J., Funk, R., Buschiazzo, D.E., 2011. Field wind erosion measurements with Big Spring Number Eight (BSNE) and Modified Wilson and Cook (MWAC) samplers. Geomorphology 129, 43–48.

Michels, K., Armbrust, D.V., Allison, B.E., Sivakumar, M.V.K., 1995. Wind and windblown sand damage to pearl millet. Agron. J. 87, 620–626. https://doi.org/10.2134/agronj1995.00021962008700040003x.

Mirzabaev, A., Wu, J., Evans, J., García-Oliva, F., Hussein, I.A.G., Iqbal, M.H., Kimutai, J., Knowles, T., Meza, F., Nedjraoui, D., Tena, F., Türkeş, M., Vázquez, R.J., Weltz, M., 2019. Desertification, in: Shukla, P.R., Skea, J., Calvo Buendia, E., Masson-Delmotte, V., Pörtner, H.-O., Roberts, D.C., Zhai, P., Slade, R., Connors, S., van Diemen, R., Ferrat, M., Haughey, E., Luz, S., Neogi, S., Pathak, M., Petzold, J., Portugal Pereira, J., Vyas, P., Huntley, E., Kissick, K., Belkacemi, M., Malley, J. (Eds.), Climate Change and Land: An IPCC Special Report on Climate Change, Desertification, Land Degradation, Sustainable Land Management, Food Security, and Greenhouse Gas Fluxes in Terrestrial Ecosystems.

Mougin, E., Demarez, V., Diawara, M., Hiernaux, P., Soumaguel, N., Berg, A., 2014. Estimation of LAI, fAPAR and fCover of Sahel rangelands (Gourma, Mali). Agr. Forest Meteorol. 198–199, 155–167. https://doi.org/10.1016/j.agrformet.2014.08.006.

Namikas, S.L., 2003. Field measurement and numerical modelling of aeolian mass flux distributions on a sandy beach. Sedimentology 50, 303–326.

Nordstrom, K.F., Hotta, S., 2004. Wind erosion from cropland in the USA: a review of problems, solutions and prospects. Geoderma 121, 157–167. https://doi.org/10.1016/j.geoderma.2003.11.012.

Okin, G.S., 2022. Where and how often does rain prevent dust emission? e2021GL095501 Geophys. Res. Lett. 49. https://doi.org/10.1029/2021GL095501.

Ouessar, M., Taâmallah, H., Ouled, B.A., 2006. Un environnement soumis à de fortes contraintes climatiques. In: Genin, D., Guillaume, H., Ouessar, M., Ouled Belgacem, A., Romagny, B., Sghaïer, M., Taâmallah, H. (Eds.), Entre Désertification Et Développement – La Jeffara Tunisienne. IRD, Tunis/Cérès Editions, Tunis/IRA, Médenine, pp. 23–32.

Panebianco, J.E., Buschiazzo, D.E., Zobeck, T.M., 2010. Comparison of different mass transport calculation methods for wind erosion quantification purposes. Earth Surf. Proc. Land. 35, 1548–1555. https://doi.org/10.1002/esp.1995.

Parolari, A.J., Li, D., Bou-Zeid, E., Katul, G.G., Assouline, S., 2016. Climate, not conflict, explains extreme Middle East dust storm. Environ. Res. Lett. 11, 114013 https://doi.org/10.1088/1748-9326/11/11/114013.

Pi, H., Webb, N.P., Huggins, D.R., Sharratt, B., 2020. Critical standing crop residue amounts for wind erosion control in the inland Pacific Northwest, USA. Catena 195, 104742. https://doi.org/10.1016/j.catena.2020.104742.

Pierre, C., Kergoat, L., Bergametti, G., Mougin, É., Baron, C., Abdourhamane Toure, A., Rajot, J.-L., Hiernaux, P., Marticorena, B., Delon, C., 2015. Modeling vegetation and wind erosion from a millet field and from a rangeland: Two Sahelian case studies. Aeolian Res. 19, 97–111. https://doi.org/10.1016/j.aeolia.2015.09.009.

Pierre, C., Kergoat, L., Hiernaux, P., Baron, C., Bergametti, G., Rajot, J.-L., Abdourhamane Toure, A., Okin, G.S., Marticorena, B., 2018. Impact of agropastoral management on wind erosion in Sahelian croplands. Land Degrad. Develop. 29, 800–811. https://doi.org/10.1002/ldr.2783.

Priestley, C.H.B., 1959. Turbulent transfer in the lower atmosphere. University of Chicago Press, Chicago (USA).

Prospero, J.M., Ginoux, P., Torres, O., Nicholson, S.E., Gill, T.E., 2002. Environmental characterization of global sources of atmospheric soil dust identified with the NIMBUS 7 Total Ozone Mapping Spectrometer (TOMS) absorbing aerosol product. Rev. Geophys. 40 https://doi.org/10.1029/2000RG000095.

Rajot, J.L., 2001. Wind blown sediment mass budget of Sahelian village land units in Niger. Bulletin de la Société Géologique de France 172, 523–531. https://doi.org/10.2113/172.5.523.

Rajot, J.L., Labiadh, M.T., Bouet, C., Pierre, C., Abdourhamane Touré, A., Henry des Tureaux, T., Ltifi, M., Sekrafi, S., 2022. Wind erosion flux, meteorology, soil roughness, and crop characteristics collected on a barley field in Dar Dhaoui (Tunisia) during 2015-2016. DataSuds, v1. https://doi.org/10.23708/URXJ25.

Santra, P., Moharana, P.C., Kumar, M., Soni, M.L., Pandey, C.B., Chaudhari, S.K., Sikka, A.K., 2017. Crop production and economic loss due to wind erosion in hot arid ecosystem of India. Aeolian Res. 28, 71–82. https://doi.org/10.1016/j.aeolia.2017.07.009.

Shahabinejad, N., Mahmoodabadi, M., Jalalian, A., Chavoshi, E., 2019a. In situ field measurement of wind erosion and threshold velocity in relation to soil properties in arid and semiarid environments. Environ. Earth Sci. 78, 501. https://doi.org/10.1007/s12665-019-8508-5.

Shahabinejad, N., Mahmoodabadi, M., Jalalian, A., Chavoshi, E., 2019b. The fractionation of soil aggregates associated with primary particles influencing wind erosion rates in arid to semiarid environments. Geoderma 356, 113936. https://doi.org/10.1016/j.geoderma.2019.11393.

Shao, Y., McTainsh, G.H., Leys, J.F., Raupach, M.R., 1993. Efficiencies of sediment samplers for wind erosion measurement. Aust. J. Soil Res. 31, 519–532.

Slama, A., Ben Salem, M., Ben Naceur, M., Zid, E., 2005. La production de céréales en Tunisie : production, effet de la sécheresse et mécanismes de résistance. Sécheresse 16, 225–229.

Squires, V.R., 2016. Dust particles and aerosols: Impact on biota “A review” (Part I). J. Range. Sci. 6, 82–91.

Stanelle, T., Bey, I., Raddatz, T., Reick, C., Tegen, I., 2014. Anthropogenically induced changes in twentieth century mineral dust burden and the associated impact on radiative forcing. J. Geophys. Res. Atmos. 119, 13526–13546. https://doi.org/10.1002/2014JD022062.

Tegen, I., Werner, M., Harrison, S.P., Kohfeld, K.E., 2004. Relative importance of climate and land use in determining present and future global soil dust emission. Geophys. Res. Lett. 31, L05105. https://doi.org/10.1029/2003GL019216.

Thameur, A., Lachiheb, B., Ferchichi, A., 2012. Drought effect on growth, gas exchange and yield, in two strains of local barley Ardhaoui, under water deficit conditions in southern Tunisia. J. Environ. Manage. 113, 495–500. https://doi.org/10.1016/j.jenvman.2012.05.026.

Udagawa, T., 1966. Variation of aerodynamical characteristics of a barley field with growth. J. Agric. Meteorol. 22, 7–14. https://doi.org/10.2480/agrmet.22.7.

Vos, H.C., Karst, I.G., Eckardt, F.D., Fister, W., Kuhn, N.J., 2022. Influence of crop and land management on wind erosion from sandy soils in dryland agriculture. Agronomy 12, 457. https://doi.org/10.3390/agronomy12020457.

Williams, G., 1964. Some aspects of the eolian saltation load. Sedimentology 3, 257–287. https://doi.org/10.1111/j.1365-3091.1964.tb00642.x.

Zhang, H., Fan, J., Cao, W., Harris, W., Li, Y., Chi, W., Wang, S., 2018. Response of wind erosion dynamics to climate change and human activity in Inner Mongolia, China during 1990 to 2015. Sci. Total Environ. 639, 1038–1050. https://doi.org/10.1016/j.scitotenv.2018.05.082.

Zhang, C.-L., Zou, X.-Y., Gong, J.-R., Liu, L.-Y., Liu, Y.-Z., 2004. Aerodynamic roughness of cultivated soil and its influences on soil erosion by wind in a wind tunnel. Soil Till. Res. 75, 53–59. https://doi.org/10.1016/S0167-1987(03)00159-4.